

Probing Single-Cell Fermentation Fluxes and Exchange Networks via pH-Sensing Hybrid Nanofibers

Original

Probing Single-Cell Fermentation Fluxes and Exchange Networks via pH-Sensing Hybrid Nanofibers / Onesto, V., Forciniti, S., Alemanno, F., Narayanankutty, K., Chandra, A., Prasad, S., Azzariti, A., Gigli, G., Barra, A., De Martino, A., De Martino, D., Del Mercato, L.L.. - In: ACS NANO. - ISSN 1936-0851. - 17:4(2023), pp. 3313-3323.
[10.1021/acsnano.2c06114]

Availability:

This version is available at: 11583/2976695 since: 2025-01-10T07:36:18Z

Publisher:

American Chemical Society

Published

DOI:10.1021/acsnano.2c06114

Terms of use:

This article is made available under terms and conditions as specified in the corresponding bibliographic description in the repository

Publisher copyright

(Article begins on next page)

Analytical Performance Estimation Methods for Modern Optical Communications systems

Giuseppe Rizzelli

Fondazione LINKS

Turin, Italy

giuseppe.rizzelli@linksfoundation.com

Roberto Gaudino

Dipartimento di Elettronica e Telecomunicazioni

Politecnico di Torino

Turin, Italy

roberto.gaudino@polito.it

Abstract—In this paper we present two different analytical tools for fast performance estimation of optical transmission systems based on both direct detection (DD) and coherent detection (CoD). We introduce the main equations used to model the communications systems and then validate the analytical results against full time domain numerical simulations. Several scenarios are considered ranging from short reach transmission over multimode fiber (MMF), to long-haul ROADM-based links and coherent detection. Our findings show an excellent agreement in every investigated condition based on realistic device parameters and advanced modulation formats typical of modern high-speed communications.

Index Terms—Performance Estimation, Fiber Optic Communications, Direct Detection, Coherent Detection

I. INTRODUCTION

Depending on the specific transmission scenario modern optical communications systems can rely on intensity modulation and direct detection (IMDD) or advanced modulation formats coupled with CoD. The former approach is used with pulse amplitude modulation (PAM) at rates up to 100 Gbps/ λ in short reach segments such as data center interconnects (DCI) where directly modulated vertical cavity surface emitting lasers (VCSELs) transmit data on MMF over distances up to a few hundred meters, or in passive optical networks (PONs) where non optically amplified transmission is achieved on a few tens of km [1], [2]. The coherent approach, on the other hand, is traditionally employed in longer reach communications such as long-haul systems over several thousands of km, coupled with advanced modulation formats and digital signal processing (DSP) at the receiver side to achieve high bit rates up to 400 Gbps/ λ [3]. However, CoD has recently moved the first steps, at least on a scientific research level, towards the shorter transmission distance segments [3]–[5], where its use is limited by the constraints imposed by complexity and cost, still to high for communications scenarios where cost-per-bit minimization is the key goal.

Management and operation of any kind of communications system at the physical layer can greatly benefit from precise knowledge of the network performance under different conditions, in the aim for efficient planning and optimization of the network capacity. This can be enabled by a fast, reliable and simple analytical tool for performance estimation, opposed to the traditional CPU-hungry and time-consuming numerical approach based on lengthy time domain simulations, which

would make infeasible the sweep of several parameters for instance in a statistical or Monte Carlo kind of performance prediction analysis.

In this paper, we present a summary of the recently developed analytical models that allow to evaluate the bit error rate (BER) of systems based on both DD or CoD. In particular, we present a model developed to analytically compute the signal-to-noise ratio (SNR) at the output of an adaptive equalizer and apply it to the two short reach scenarios of a 100 Gbps/ λ PON architecture using 4-PAM transmission and an avalanche photodiode (APD) at the receiver [6], and a 400G shortwave wavelength division multiplexing (SWDM) scheme using 4-PAM modulated VCSELs and multimode fiber propagation for DCI solutions [2]. Moreover, we show a similar model for the SNR computation of polarization multiplexed CoD-based systems that can be described through a generic frequency and polarization dependent transfer function matrix [7]. We apply this model to the traditional long-haul core network scenario where the transmitted signal crosses and is filtered by a cascade of reconfigurable optical add-drop multiplexers (ROADMs), and to a more unusual scenario of a MMF-based transmission employing coherent detection and advanced modulation schemes [5]. In both these models the BER of the system can be derived through the well-known equations relating BER and SNR, via the *erfc* function, for a specific modulation format.

The remainder of this manuscript is organized as follows: in Section II we introduce the analytical model in the IMDD transmission scenario and show its validation in terms of SNR and BER compared to the results obtained through full time domain simulations. We then apply the model to the PON and SWDM architecture and discuss the outcome. In Section III we describe the analytical tool in the CoD-based communications and apply it to the statistical analysis of long-haul and coherent-over-MMF (Coh-MMF) systems showing the distribution of the SNR estimation error. Lastly, in Section IV we discuss the main findings of our work and draw some conclusions.

II. PREDICTION OF IMDD TRANSMISSION PERFORMANCE

The developed model is based on the work presented in [8] and detailed in [6], [9], where the Author estimates the SNR at

the output of a feed-forward equalizer (FFE) and of a decision feedback equalizer (DFE) as

$$SNR_{FFE} = \frac{1}{T \cdot \int_{-\frac{1}{2T}}^{\frac{1}{2T}} \frac{1}{\overline{SNR}(f)+1} df} - 1 \quad (1)$$

$$SNR_{DFE} = e^{T \cdot \int_{-\frac{1}{2T}}^{\frac{1}{2T}} \log[\overline{SNR}(f)+1] df} - 1 \quad (2)$$

where $\overline{SNR}(f)$ is the spectral $SNR(f)$ folded on a bandwidth equal to the symbol rate (due to the analog-to-digital conversion process in front of the equalizer). In the specific case of PAM-4 modulation, a typical format considered in recent standardization effort for modern high capacity IMDD solutions, we can write

$$SNR(f) = \frac{5}{36} \cdot \frac{T \cdot (OMA_{TX}^{outer})^2 \cdot |H_T(f)|^2 \cdot |H_{ch}(f)|^2}{S_N(f)} \quad (3)$$

where OMA_{TX}^{outer} is the outer Optical Modulation Amplitude (OMA) in W, T is the symbol period, $H_{ch}(f)$ is the linear channel transfer function, $H_T(f)$ is the transfer function of the transmitter shaping filter and $S_N(f)$ is the power spectral density (PSD) at the equalizer input (expressed in W^2/Hz), which we write as the sum of the (statistically independent) contribution of three noise sources

$$S_N(f) = S_{RIN}(f) \cdot |H_{ch}(f)|^2 + S_{shot}(f) + S_{th}(f) \quad (4)$$

where $S_{th}(f)$ is the PSD of the additive thermal noise, $S_{RIN}(f)$ is the PSD of the relative intensity noise (RIN) and $S_{shot}(f)$ is the PSD of the shot noise. Since our approach is defined in the frequency domain we cannot analytically take into account the instantaneous time dependence of the noise level. Thus we describe $S_{RIN}(f) = k_{RIN} \cdot P_{TX}^2$ and $S_{shot} = k_{shot} \cdot \overline{P_{RX}}$, where P_{TX}^2 is the average transmitted optical power squared, $k_{RIN} = RIN_{coeff}/2$ is a proportionality factor that depends on the RIN coefficient RIN_{coeff} expressed in $1/Hz$, $\overline{P_{RX}}$ is the average received optical power and $k_{shot} = 2G^2 F q R^{-1}$ is a proportionality factor that depends on the photodetector excess noise figure F , the photodetector gain G (when considering avalanche photodetection, whereas for a PIN photodiode $G = F = 1$), the photodiode responsivity R and the electron charge q .

As a first validation of the model Fig. 1 shows a comparison of the analytical results against the performance returned by time domain simulations of a 25 GBaud PAM-4 system as a function of the ratio between the 3dB bandwidth B_{3dB} of a supergaussian filter describing the channel transfer function $H_{ch}(f)$ and the symbol rate R_s . We assume a rectangular shaping at the transmitter and also vary the order of the supergaussian filter. Fig. 1a shows a nearly perfect estimation of the SNR at the output of both FFE and DFE equalizer, whereas Fig. 1b highlights also an excellent match in terms of BER calculated in the simulations through error counting.

We can use the proposed model to study any transmission system that can be described by a cascade of linear transfer functions. For instance, Fig. 2 shows a simplified block

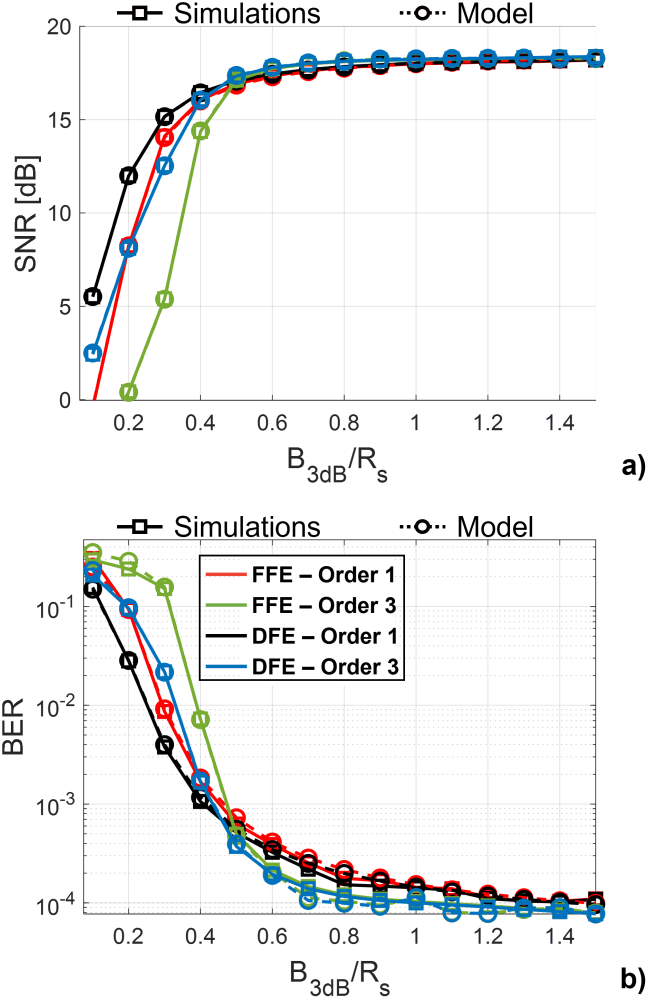


Fig. 1. a) SNR and b) BER obtained through time domain simulations (solid, squares) and through the proposed analytical model (dashed, circles) as a function of the ratio between the supergaussian filter 3 dB bandwidth B_{3dB} and the symbol rate R_s for a 25 GBaud 4-PAM system, using both FFE (red and green) and DFE (black and blue) equalization. The supergaussian filter order is 1 for black and red curves and 3 for blue and green curves. The legend in b) applies to a) as well.

diagram of a PON with a 50G-class APD at the receiver side with $G = 10$ dB, $F = 4.3$ dB and $R = 0.7$ A/W. Fig. 3 shows the SNR obtained through the analytical approach and by time domain simulations for a 50 GBaud PAM-4 transmission, highlighting again a remarkable agreement for different extinction ratio (ER) values and for both back-to-back and transmission over 25 km with FFE equalization. When considering the 25 km single mode fiber (SMF) link we assumed propagation in the O-band and considered a 3.85 ps/nm·km chromatic dispersion (CD) coefficient D and used the small signal approximation [10] to describe the electrical-to-electrical transfer function of the system under chromatic dispersion effect only as

$$H_{CD}(f) = \cos \left[\pi c D L \left(\frac{f}{f_c} \right)^2 \right] \quad (5)$$

where L is the fiber length and f_c is the central frequency of the optical signal.

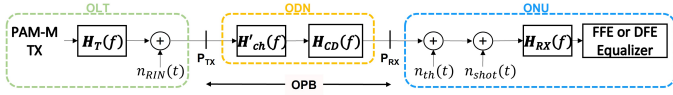


Fig. 2. Simplified scheme of the PON under investigation. OLT: optical line terminal; ODN: optical distribution network; ONU: optical network unit.

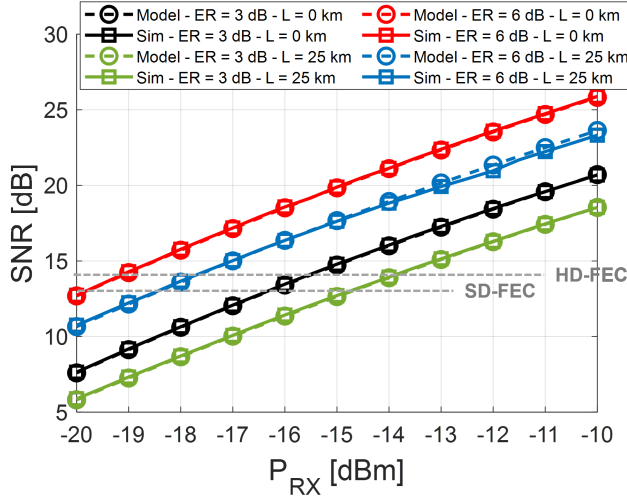


Fig. 3. a) SNR obtained through time domain simulations (solid, squares) and through the proposed analytical model (dashed, circles) as a function of the received optical power using 50 GBaud 4-PAM with FFE equalization in back-to-back (black, green) and with 25 km SMF in O-band (red, blue). Transmitted power is 11 dBm, ER is 3 dB (black, red) or 6 dB (green, blue).

We assumed 11 dBm transmitted optical power, thus the only configuration that enables 29 dB optical power budget (OPB), as required by class N1 PON, is with 6 dB ER and soft decision forward error correction (SD-FEC). The use of hard decision forward error correction (HD-FEC), on the other hand, allows to obtain sufficient OPB only in back-to-back.

Fig. 4 shows another transmission scenario that can be analyzed through our analytical model. We consider the 4λ 100 Gbps/ λ PAM-4 SWDM VCSEL-MMF system with 20233 MMFs (16467 OM3 and 3766 OM4) coupled with 8 VCSELs presented in [2]. The bit rates R_b are 106.25 Gbps when using a KP4 FEC with bit error rate threshold $BER_T = 2 \cdot 10^{-4}$ and 110.35 Gbps when a stronger enhanced-FEC (E-FEC) with $BER_T = 4 \cdot 10^{-3}$ is used. Numerical and analytical calculations are applied to the setup in Fig. 4, where $H_{TX}(f)$ represent the shaping filter at the transmitter (rectangular in this specific analysis), $H_{VCSEL}(f)$ is the measured transfer function of the VCSEL with 25 GHz 3dB cut-off frequency, $H_{MMF}(f)$ is the transfer function calculated as in [11] for the 161864 VCSEL-MMF combinations at the 4 SWDM wavelengths for different MMF lengths, ranging from 30 m to 400 m. Lastly, $H_{RX}(f)$ is the frequency response of the photodiode described as an 8th order Butterworth filter with 26 GHz 3-dB cutoff frequency. Moreover, Fig. 4 shows where the

$n_{RIN}(t)$, $n_{shot}(t)$ and $n_{th}(t)$ contributions, respectively from RIN, shot and thermal noise are added in the simulations.

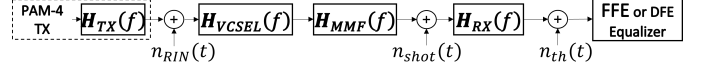


Fig. 4. Block diagram of the simulated VCSEL-MMF link.

Fig. 5 shows the maximum reach for 99% of the tested links predicted by the model and that obtained through time domain simulations, for both FFE and DFE and for the OM3 and OM4 fiber sets. The time domain simulations always underestimate the system performance due to a non-perfect optimization of the equalizer parameters such as step size and number of taps. The model, on the other hand, assumes ideal infinitely long equalization and can thus be considered as an upper bound. Moreover, the estimation error is greater when considering DFE equalization due to the well-known error propagation effect that cannot be taken into account in the model.

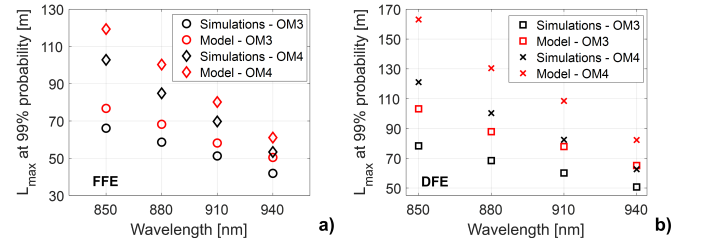


Fig. 5. Time-domain (black) and analytical model (red) prediction of maximum reach at the four SWDM wavelengths for a) FFE and b) DFE considering OM3 (circles, squares) and OM4 (diamonds, crosses) fibers and KP4 FEC (106.25 Gbps bit rate).

III. PERFORMANCE ESTIMATION OF COHERENT SYSTEMS

We developed a similar model to the one presented in Section II also for the coherent communications case [7]. This version is still based on [8], but modified to take into account generic frequency and polarization dependence. The block diagram describing our approach is depicted in Fig. 6 where $\mathbf{H}_{sn}(f) = \mathbf{H}_s(f) \cdot \mathbf{H}_n(f)^{-1}$ is the cascade of a linear generic $[2 \times 2]$ frequency and polarization dependent transfer function $\mathbf{H}_s(f)$, acting on the transmitted PM-QAM signal and representing the propagation link, and the noise-whitening matrix $\mathbf{H}_n^{-1}(f)$, inverse of the transfer function applied to the noise component, that allows to account for a generic polarization-dependent PSD for the additive noise. Both $\mathbf{H}_s(f)$ and $\mathbf{H}_n(f)$ are assumed to be invertible.

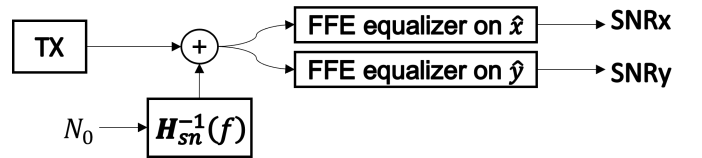


Fig. 6. Block diagram of the CoD model.

In this equivalent model the \hat{x} and \hat{y} QAM components on the two polarizations are separated and the frequency dependent $SNR(f)$ can be independently evaluated on the two polarizations. The received field after the equalizer on the two polarizations is

$$\begin{bmatrix} E^x(f) \\ E^y(f) \end{bmatrix}_{eq} = \begin{bmatrix} E^x(f) \\ E^y(f) \end{bmatrix}_{TX} + \mathbf{K}(f) \cdot \begin{bmatrix} n^x(f) \\ n^y(f) \end{bmatrix} \quad (6)$$

where $n^x(f)$ and $n^y(f)$ are additive white noise components with PSD N_0 and

$$\mathbf{K}(f) = \mathbf{H}_{sn}(f)^{-1} = \begin{bmatrix} K^{xx}(f) & K^{xy}(f) \\ K^{yx}(f) & K^{yy}(f) \end{bmatrix} \quad (7)$$

Converting Eq. 6 in terms of PSD we have

$$\begin{bmatrix} P^x(f) \\ P^y(f) \end{bmatrix}_{eq} = \begin{bmatrix} P^x(f) \\ P^y(f) \end{bmatrix}_{TX} + \begin{bmatrix} |K^{xx}(f)|^2 + |K^{xy}(f)|^2 \\ |K^{yx}(f)|^2 + |K^{yy}(f)|^2 \end{bmatrix} \cdot N_0 \quad (8)$$

and the $SNR(f)$ on the two polarizations is

$$SNR_x(f) = \frac{P_{TX}^x(f)}{(|K^{xx}(f)|^2 + |K^{xy}(f)|^2) \cdot N_0} \quad (9)$$

$$SNR_y(f) = \frac{P_{TX}^y(f)}{(|K^{yx}(f)|^2 + |K^{yy}(f)|^2) \cdot N_0}$$

We now apply this analytical tool to the study of two different communications scenarios. The first one is the common transmission of a PM-QAM signal through a cascade of erbium doped fiber amplifiers (EDFAs) and ROADMS, typical for core and metro networks. We consider N ROADMs, each containing 2 wavelength selective switches (WSS) described by a Super-Gaussian (SG) profile of order 6 and we assume polarization dependent loss (PDL) $PDL_{dB} = 1$ dB introduced by each individual WSS. Both $\mathbf{H}_s(f)$ and $\mathbf{H}_n(f)$ are generated equally with a supergaussian profile and with the same PDL but different unitary Jones matrices are applied to account for random fiber birefringence. Each filter has a 75 GHz bandwidth and the signal is a 64 GBaud PM-16QAM with raised cosine shaping and 0.2 roll-off factor. Considering a 27% overhead FEC, the net bit rate in our numerical example is about 400 Gbit/s. To emulate non-perfect WSS alignment, the central frequency of each filter varies randomly in a range within $\pm 5\%$ of the filter bandwidth. Fig. 7 shows the probability density function (pdf) of the difference in dB between the SNR predicted by the analytical model and that obtained through time domain simulation on 3000 randomly generated Jones matrices in a Monte-Carlo analysis. The average estimation error is about 0.1 dB and values in excess of 0.2 dB or -0.05 dB can be considered negligible.

The second application scenario of the proposed analytical model is related to the exploitation of CoD in the DCI segment usually relying on DD. In [4], [5] we analyze an MMF-based transmission with PM-16QAM modulation and coherent detection. Coherent receivers are inherently coupled to standard SMF both at the transmitter and receiver side, thus we indicate the resulting link as SMF-MMF-SMF coherent

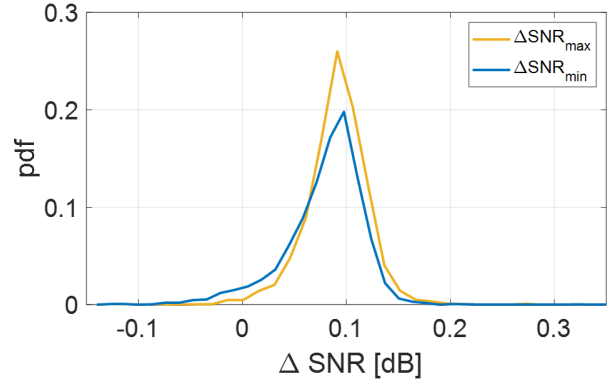


Fig. 7. Probability density function of the error between the analytical model and the time domain simulator for both the maximum (yellow) and minimum (blue) SNR in the ROADM study case, for 3000 runs.

system. In these systems propagation can be described by the following [2x2] frequency-dependent transfer function matrix:

$$\mathbf{H}(f) = \sum_{j=0}^{M-1} \rho_j^{in} \mathbf{J}_j e^{-j2\pi f \tau_j} \rho_j^{out} \quad (10)$$

where M is the total number of MMF modes, j is the index of the j th MMF mode, ρ_j^{in} is the coupling coefficient between the LP₀₁ SMF mode and the j th MMF mode, ρ_j^{out} is the coupling coefficient between the j th MMF mode and the SMF LP₀₁ mode that can be calculated using the analytical model presented in [12], \mathbf{J} is the unitary random Jones matrix that takes into account "per mode" fiber birefringence and τ_j is the modal delay of the j th mode inside the MMF. Fig. 8 shows the distribution of the difference in dB between the SNR predicted by the analytical model and that obtained through time domain simulation on 3000 randomly generated Jones matrices in a Monte-Carlo analysis. Similarly to the previous case the average absolute estimation error is about 0.1 dB, but in this case the maximum values can be slightly higher due to very pronounced frequency dips in the transfer function, where the invertible matrix assumption might become inaccurate.

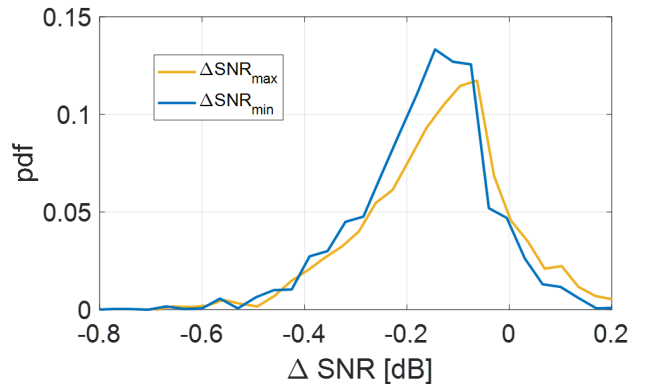


Fig. 8. Probability density function of the error between the analytical model and the time domain simulator for both the maximum (yellow) and minimum (blue) SNR in the SMF-MMF-SMF study case, for 3000 runs.

IV. CONCLUSION

We have presented two analytical tools for the prediction of communications systems performance relying on intensity modulation and direct detection or advanced modulation and coherent detection. The SNR at the output of adaptive equalizers such as FFE or DFE can be computed in a fast and accurate way resulting in more than 300 times reduction in estimation time compared to CPU-hungry time domain simulations. Our findings show a very high level of accuracy in several different transmission scenarios with estimation errors as low as 0.1 dB on average.

ACKNOWLEDGMENT

This work was carried out under a research contract with Cisco Photonics and in the PhotoNext initiative at Politecnico di Torino. www.photonext.polito.it.

REFERENCES

- [1] P. Torres-Ferrera, G. Rizzelli, H. Wang, V. Ferrero and R. Gaudino, "Experimental Demonstration of 100 Gbps/ λ C-Band Direct-Detection Downstream PON Using Non-Linear and CD Compensation with 29 dB+ OPL Over 0 Km–100 Km," in *J. Lightwave Technol.*, vol. 40, no. 2, pp. 547-556, 2022.
- [2] P. Torres-Ferrera et al., "Statistical Analysis of 100 Gbps per Wavelength SWDM VCSEL-MMF Data Center Links on a Large Set of OM3 and OM4 Fibers," in *J. Lightwave Technol.*, vol. 40, no. 4, pp. 1018-1026, Feb. 15, 2022.
- [3] G. Rizzelli, A. Nespola, S. Straullu, F. Forghieri and R. Gaudino, "Scaling Laws for Unamplified Coherent Transmission in Next-Generation Short-Reach and Access Networks," *J. Lightwave Technol.*, vol. 39, no. 18, pp.5805-5814, 2021.
- [4] G. Rizzelli, F. Forghieri and R. Gaudino, "Experimental Demonstration of Real-Time 400G Coherent Transmission Over 300m OM3 MMF," in *Proc. OFC*, San Diego, CA, USA, 2022.
- [5] G. Rizzelli, P. Torres-Ferrera, F. Forghieri, A. Nespola, A. Carena and R. Gaudino, "Coherent Communication Over Multi Mode Fibers for Intra-Datacenter Ultra-High Speed Links," in *Journal of Lightwave Technology*, vol. 40, no. 15, pp. 5118-5127, 1 Aug.1, 2022.
- [6] G. Rizzelli, P. Torres-Ferrera and R. Gaudino, "An Analytical Model for Performance Estimation in High-Capacity IMDD Systems", in *arXiv*, vol. 2304, no. 10834, 2023.
- [7] G. Rizzelli, P. Torres-Ferrera and R. Gaudino, "An Analytical Model for Coherent Transmission Performance Estimation after Generic Jones Matrices," in *J. Lightwave Technol.*, doi: 10.1109/JLT.2023.3242329.
- [8] Robert F.H. Fischer, "Linear Equalization," in *Precoding and Signal Shaping for Digital Transmission*, New York, NY, USA: Wiley-Interscience, 2002, ch. 2, sec. 2.2.4, pp. 35-43.
- [9] G. Rizzelli, P. Torres-Ferrera and R. Gaudino, "An Analytical Model for Performance Estimation in Modern High-Capacity IMDD Systems," unpublished .
- [10] J. Wang and K. Petermann, "Small signal analysis for dispersive optical fiber communication systems," in *Journal of Lightwave Technology*, vol. 10, no. 1, pp. 96-100, Jan. 1992.
- [11] J. M. Castro, R. Pimpinella, B. Kose and B. Lane, "Investigation of the Interaction of Modal and Chromatic Dispersion in VCSEL–MMF Channels," *Journal of Lightwave Technology*, vol. 30, no. 15, pp. 2532-2541, Aug.1, 2012, doi: 10.1109/JLT.2012.2203351.
- [12] A. Amphawan, F. Payne, D. O'Brien and N. Shah, "Derivation of an Analytical Expression for the Power Coupling Coefficient for Offset Launch Into Multimode Fiber," *IEEE/OSA Journal of Lightwave Technology*, vol. 28, no. 6, pp. 861-869, March 15, 2010, doi: 10.1109/JLT.2009.2034475.